

Mixed Ligand Palladium(II) Complex with NS-Bidentate S-Allyldithiocarbazate Schiff Base: Synthesis, Spectral Characterization, Crystal Structure and Decoding Intermolecular Interactions with Hirshfeld Surface Analysis

Takjoo, Reza^{*,a} Takjoo, Rozita^b Yazdanbakhsh, Mohammad^c
Aghaei kaju, Amir^d Chen, Yaguang^e

^a Department of Chemistry, Faculty of Science, Islamic Azad University-Mashhad Branch, Mashhad, Iran

^b Shirvan Azad University-Shirvan Branch, Shirvan, Iran

^c Department of Chemistry, School of Sciences, Ferdowsi University of Mashhad, Mashhad 91779-1436, Iran

^d Department of Chemistry, Research Institute of Sciences & Food Technology, Khorasan Science & Technology Park, Mashhad, 91735-139, Iran

^e Faculty of Chemistry, Northeast Normal University, 138 Renmin Street, Changchun 130024, China

A new mixed ligand palladium(II) complex with bidentate NS-donor chelate, [PdCl(PPh₃)L] (L: *S*-allyl β -*N*-(benzylidene)dithiocarbazate), has been prepared and characterized using single crystal X-ray diffraction and spectroscopic (electronic, IR, ¹H NMR and ¹³C NMR) techniques. The shorter Pd—P bond distance, 2.255(7) Å, than the sum of the single bond radii for palladium and phosphorus (2.41 Å), showed partial double bond character. Visualizing and exploring the crystal structure using Hirshfeld surface analysis showed the presence of $\pi\cdots\pi$, N $\cdots\pi$, C—H $\cdots\pi$, Cl \cdots H and weak C—H \cdots S interactions as most important intermolecular interactions in the crystal lattice, which are responsible to extension of the supramolecular network of the compound and stabilization of the crystal structure.

Keywords palladium(II), *S*-allyldithiocarbazate, X-ray crystal structure, Hirshfeld surface analysis

Introduction

Transition metal chelates of hard-soft nitrogen-sulfur dithiocarbazic acid, its *S*-alkyl/aryl esters and their Schiff bases have been studied, mainly due to their potential anticancer,¹ antifungal,² antiamoebic³ and insecticidal⁴ activities. Various transition and innertransition metal complexes with SN donor Schiff bases play an important role in biological systems and represent interesting models for metalloenzymes that efficiently catalyze the reduction of dinitrogen and dioxygen.^{5,6} Furthermore, macrocyclic derivatives of these Schiff bases were found to have many fundamental biological functions, such as photosynthesis and transport of oxygen in respiratory systems of mammalian.⁷ Coordination chemistry of Pd(II) Schiff bases has been appealing for research in recent years due to its application to several catalytic and biological systems.^{3,8} Although, plenty of studies have been done on the complexes of Pd(II) with dithiocarbazic acid,⁹ Schiff bases of *S*-methyl,^{3,8} *S*-benzyl^{3,10} and *S*-acetyl^{3a} dithiocarbazate and other *N*-substituted derivatives of *S*-methyl dithiocarbazate¹¹ have been reported, few complexes based on *S*-allyl-

dithiocarbazate can be found. Herein, as a part of our longstanding efforts in the synthesis of SN donor Schiff base complexes,¹² we report the synthesis, structure and spectral characterization of new mixed ligand Pd(II) complex [PdCl(PPh₃)L] (L: *S*-allyl β -*N*-(benzylidene)-dithiocarbazate) using the bidentate ligand "*S*-allyl-dithiocarbazate" Schiff base.

McKinnon *et al.*¹³ have recently presented a detailed review of the application of the Hirshfeld surface¹⁴ to explain and describe a wide variety of molecular crystal structures, and it was clear from the work that graphical tools based on the Hirshfeld surface and the associated two dimensional (2D) fingerprint plot¹⁵ offered considerable promise for exploring packing modes and intermolecular interactions in molecular crystals.

In this paper, according to Hirshfeld surface-based tools, we use CrystalExplorer to decoding of intermolecular interactions in crystal network. The 3D shape and curvature surfaces and breakdown of fingerprint plots¹⁶ (existing new techniques and tools based on the Hirshfeld surface and already incorporated in CrystalExplorer computer program) were applied to visual-

* E-mail: rezatakjoo@yahoo.com; Tel.: 098-0511-6082637

Received May 1, 2009; revised August 28, 2009; accepted October 9, 2009.

izing and exploring intermolecular interactions in crystal lattice.

Experimental

All chemicals used for the ligand and the complex preparation have analytical quality, which were used without further purification. Spectrograde solvents were used for spectral measurements. Deuterated solvents CDCl₃ and DMSO-*d*₆ were used for NMR measurements.

Physical measurements

¹H NMR and ¹³C NMR spectral measurements were performed on a Bruker BRX 100 AVANCE spectrometer and Bruker BRX 500 AVANCE 500 MHz spectrometer (CDCl₃ or DMSO-*d*₆). All chemical shifts were reported downfield from standards. Elemental analyses were carried out by using a Thermo Finnigan Flash Elemental Analyzer, model 1112EA and a Shimadzu AA-670 atomic absorption spectrometer. IR spectra (KBr pellets) were recorded on a Buck-500 Scientific infrared spectrophotometer (4000–600 cm^{−1}). Electronic spectra of the complexes in methanol solution (ca. 25 °C) were recorded on an Agilent 8453 single beam UV-Vis spectrophotometer (250–900 nm). The mass spectra were recorded on a Varian CH-7 instrument at 70 eV. Melting point was determined using an electrothermal digital melting point apparatus.

Crystallographic analysis

Experimental parameters pertaining to single crystal X-ray analysis are given in Table 1. Data were collected on an orange cubic crystal mounted and centered on a glass capillary, which was put on a Smart-Apex CCD (Bruker-AXS) diffractometer equipped with graphite monochromated Mo Kα radiation (λ = 0.71073 Å). The final unit cell was determined from 8603 reflections in the range of 1.85° < θ < 28.31°. The diffraction data were collected at 296 K with φ- and ω-scan techniques. The structure was solved by direct methods and refined by full-matrix least squares based on *F*² with weight $w = 1/[\sigma^2(F_o^2) + (0.0362P)^2 + 1.2160P]$ where $P = (F_o^2 + 2F_c^2)/3$ using the SHELXTL-97 software.¹⁷ All non-hydrogen atoms were refined with anisotropic displacement parameters and hydrogen atoms were placed isotropically on calculated positions. Refinement of *F*² was against all reflections. The weighted *R*-factor *wR* and goodness of fit *S* are based on *F*², conventional *R*-factors *R* are based on *F*, with *F* set to zero for negative *F*². The threshold expression of *F*² > 2σ(*F*²) was used only for calculating *R*-factors (geometrical treated) *etc.*, and is not relevant to the choice of reflections for refinement. *R*-factors based on *F*² are statistically about twice as large as those based on *F*, and *R*-factors based on all data will be even larger.

Crystallographic information has been deposited with the Cambridge Crystallographic Data Centre

Table 1 Crystallographic data for the title compound

Formula	C ₂₉ H ₂₆ ClN ₂ PPdS ₂
Formula weight	639.51
<i>T</i> /K	296(2)
Crystal system	Triclinic
Crystal size/mm ³	0.151 × 0.121 × 0.082
Space group	<i>P</i> -1
<i>a</i> /Å	10.2376(7)
<i>b</i> /Å	11.3048(8)
<i>c</i> /Å	12.5828(8)
α/(°)	90.5660(10)
β/(°)	100.7140(10)
γ/(°)	102.5310(10)
<i>V</i> /Å ³	1394.87(16)
<i>Z</i>	2
<i>D</i> _{calc} /(Mg•m ^{−3})	1.475
μ/mm ^{−1}	0.987
<i>F</i> (000)	620
θ range/(°)	1.85 to 28.31
Index ranges	−13 ≤ <i>h</i> ≤ 13, −14 ≤ <i>k</i> ≤ 13, −10 ≤ <i>l</i> ≤ 16
Reflections collected	8603
Data/restraints/parameters	6212/2/325
Goodness-of-fit on <i>F</i> ²	1.025
Radiation (λ/Å)	Mo Kα (0.71073)
Independent reflections	6212 [<i>R</i> _(int) = 0.0144]
Completeness to θ = 28.31°	89.4%
Absorption correction	Semi-empirical from equivalents
Refinement method	Full-matrix least-squares on <i>F</i> ²
Final <i>R</i> indices [for 4865 rfln. with <i>I</i> > 2σ(<i>I</i> ₀)]	<i>R</i> ₁ = 0.0394, <i>wR</i> ₂ = 0.0870
<i>R</i> indices (all data)	<i>R</i> ₁ = 0.0555, <i>wR</i> ₂ = 0.0952
Largest diff. peak and hole	0.710 and −0.695 e.Å ^{−3}

(CCDC number = 671381). Copies of the data can be obtained free of charge via www.ccdc.cam.ac.uk/conts/retrieving.html (or from the Cambridge Crystallographic Data Centre, 12 Union Road, Cambridge CB2 1EZ, UK; fax: 0044 1223 336033; or deposit@ccdc.cam.ac.uk).

Preparation of *S*-allyl β-*N*-(benzylidene)dithiocarbazate (HL)

This compound was prepared and characterized by following, a previously published procedure.^{12b} To an ethanolic solution (30 mL) of 5 mL (0.1 mol) of hydrazine hydrate and 5.6 g (0.1 mol) KOH, was added dropwise a solution of 6.1 mL (0.1 mol) of carbon disulfide in an ice bath. After 30 min 8.6 mL (0.1 mol) of allyl bromide was added. The solution was stirred con-

tinuously at 5 °C for 1 h. The ethanolic solution (25 mL) of benzaldehyde (11.1 mL, 0.1 mol) was added to this mixture and heated with continuous stirring. After 15 min, a yellow product was separated by filtration, washed with water and dried in vacuum. HL was recrystallized from ethanol. Yield 49.5% (based on benzaldehyde), m.p. 137 °C. UV-Vis (CH₂Cl₂) λ_{max} /nm [ϵ /(dm³·mol⁻¹·cm⁻¹)]: 240 (36450), 334 (9640) (intra-ligand transition); ¹H NMR (DMSO-*d*₆, 500 MHz) δ : 3.90 (d, *J* = 7 Hz, 2H, SCH₂), 5.24 (dd, *J* = 18, 10 Hz, 2H, CH₂), 5.87–5.96 (m, H, CH), 7.45 (dd, *J* = 2, 4 Hz, 3H, *o,p*-C₆H₅), 7.71 (dd, *J* = 2, 4 Hz, 2H, *o*-C₆H₅), 8.24 (s, 1H, CH = N), 13.34 (s, 1H, NH); ¹³C NMR (DMSO-*d*₆, 500 MHz) δ : 196.44 (C=S), 146.56 (CH = N), 133.28 [C(6)], 133.16 (*p*-C₆H₅), 130.77 (CH), 128.95 (*o*-C₆H₅), 127.42 (*m*-C₆H₅), 118.45 (CH₂), 35.98 (SCH₂); IR (KBr) ν : 751 δ (out-of-plane of CH, phenyl deformation), 1025 ($\nu_{\text{N-N}}$), 1097 ($\nu_{\text{C-S}}$), 1609 ($\nu_{\text{C-N}}$), 2962 ($\nu_{\text{CH aliphatic}}$), 3109 ($\nu_{\text{N-H}}$) cm⁻¹; MS *m/z*: 236, 162, 118, 104, 92, 77, 41 and 28. Anal. calcd for HL (C₁₁H₁₂N₂S₂): C 55.90, H 5.12, N 11.85, S 27.13; found C 55.96, H 5.00, N 11.85, S 28.26.

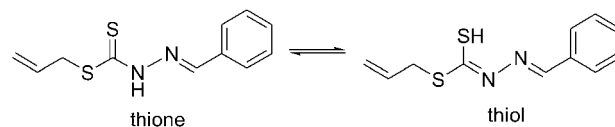
Preparation of chloro-[allyl-2-(phenylmethylidene)-1-hydrazinecarbodithioato-*N,S*]-[triphenylphosphine]-palladium(II) ([PdCl(PPh₃)L])

A solution of HL (0.236 g, 1 mmol) and triphenylphosphine (0.262 g, 1 mmol) in acetonitrile (15 mL) was added to a solution of K₂PdCl₄ (0.362 g, 1 mmol) in water under magnetic stirring for 20 min. An orange solid product was filtered, washed with water, dried in vacuum and recrystallized from acetonitrile. Yield 51% (based on HL), m.p. 198 °C; UV-Vis (CH₂Cl₂) λ_{max} /nm [ϵ /(dm³·mol⁻¹·cm⁻¹)]: 242 (18240), 262 (26460) (intra-ligand transition); 312 (29000) (LMCT), 444 (500) (d-d); ¹H NMR (CDCl₃, 100 MHz) δ : 3.76 (d, *J* = 7 Hz, 2H, SCH₂), 5.18 (dd, *J* = 17, 10 Hz, 2H, CH₂), 5.70–5.97 (m, 1H, CH), 7.25–8.19 (m, 20H, aromatic rings), 8.87 (d, *J* = 4 Hz, 1H, CH = N); IR (KBr) ν : 754 (out-of-plane of CH, phenyl deformation), 1011 ($\nu_{\text{N-N}}$), 1582 ($\nu_{\text{C-N}}$), 1487, 1091 & 688 (for PPh₃) cm⁻¹. Anal. calcd for C₂₉H₂₆ClN₂PPdS₂: C 54.47, H 4.10, N 4.38, S 10.03, Pd 16.64; found C 52.98, H 3.97, N 4.34, S 9.69, Pd 16.21.

Results and discussion

The Schiff base *S*-allyl β -*N*-(benzylidene)dithiocarbamate [HL], was readily prepared by condensation of benzaldehyde with *S*-allyldithiocarbamate in ethanol solution as a fluffy pale-yellow crystalline solid. Like all other Schiff bases derived from *S*-alkyl/aryl dithiocarbamates, the HL is also capable of exhibiting thione-thiol tautomerism since they contain the thioamide, —NH—C(S)S— functional group (Scheme 1).^{12b} The thione group is relatively unstable and tends to convert to the more stable C—S bond by enolization, if there is at least one proton adjacent to the thione group.

Scheme 1 The thione and thiol tautomeric forms of the Schiff base (HL)



It has two potential donor atoms available for coordination with a metal ion. The reaction of HL with K₂PdCl₄ and triphenylphosphine at a molar ratio of 1 : 1 : 1 gave an orange complex, [PdCl(PPh₃)L]. The complex was characterized by ¹H NMR, IR and UV-Vis spectroscopies, besides elemental analyses, and its molecular structure was determined by single-crystal X-ray analyses.

Infrared spectra

The HL can exhibit thione-thiol tautomerism. In the solid state the absence of $\nu(\text{S—H})$ at *ca.* 2570 cm⁻¹ from the IR spectra shows that only the thione form exists, as shown in Scheme 1.¹⁸ The band at 3097 cm⁻¹ and the strong intensity band at 1025 cm⁻¹ were attributed to $\nu(\text{N—H})$ and $\nu(\text{N—N})$ vibration modes, respectively. The $\nu(\text{N—H})$ and $\nu(\text{C=S})$ are missing from the IR spectra of complex, suggesting that the ligand exists in complex in deprotonated thione form, which is further supported by the red shift of the $\nu(\text{C=N})$ band for the complex with respect to the free ligand, indicating shorter C=N bond lengths in free ligand. The bands at 1487, 1090 and 688 cm⁻¹ were attributed to triphenylphosphine.¹⁹

Electronic spectra

The electronic spectra of the ligand and complex have been recorded in chloroform as solvent and were listed in experimental section. For free ligand two absorptions, 240 and 334 nm, in the ultraviolet region is assignable to intra-ligand orbital transitions. As the same, two bands appeared around 242 and 262 nm have been assigned to intra-ligand transition in the complex.

In addition, charge transfer band is appeared at approximately 312 nm. This intense band may be assigned to a combination S→Pd(II), N→Pd(II), P→Pd(II) and Cl→Pd(II) charge transfer bands.

In the visible region of the square planar palladium complexes, three spin-allowed d-d transitions were considered.²⁰ These transitions were expected to correspond to the transitions ¹A_{1g}→¹A_{2g}, ¹A_{1g}→¹B_{1g} and ¹A_{1g}→¹E_g but the presence of sulfur covers these bands, because of its very intense charge transfer band, and the band ¹A_{1g}→¹E_g in the range of 444 nm was merely observed.

¹H NMR, ¹³C NMR and EI mass spectra

The d⁸ square planar palladium(II) complexes give well resolved NMR spectra, which confirm the nature of the binding. In ¹H NMR spectrum of the free ligand, the extreme downfield is assignable to NH, which disap-

pears on coordination and deuteration. The aromatic portion is sharply divided to two parts: the downfield portion and the upper field part which are referred to 2,3,4-H and 1,5-H, respectively. The singlet at δ 8.24 was assigned to the imine proton. The ^1H NMR spectrum of the ligand revealed existence of the thione form as a single form. In the complex, downfield shifts were also observed for the imine hydrogen, indicating decreased electron density on coordination. However, all of allyl hydrogens were shifted upfield, which may be considered for increasing conjugation following complexation.

The ^1H NMR spectrum of the complex showed a series of multiple overlapping signals for aromatic protons in δ 7.25–8.19. The azomethine proton resonance is splitted into a doublet maybe due to the splitting of CH resonance by protons of phenyl group occurring in δ 8.85–8.89.¹⁹

The ^{13}C NMR spectrum of the ligand showed a signal at downfield δ 196.44 corresponding to the thioamide carbon, which was found in DMSO at room temperature. In addition, the azomethine carbon signal of the ligand appeared at δ 146.56. The SCH_2 , CH and CH_2 carbons in the allyl group show signals at δ 35.98, 130.77 and 118.45, respectively. The signals of the carbons on the phenyl ring appear in δ 127.42 to 133.28.

Crystal structure

The reaction of K_2PdCl_4 and PPh_3 with $[\text{H}(\text{L})]$ at a 1 : 1 : 1 molar ratio afforded complex of the type $[\text{PdCl}(\text{PPh}_3)\text{L}]$ (where $\text{L} = \text{NS}$ bidentate *S*-allyl β -*N*-(benzylidene)dithiocarbazate ligand). The single crystals of $[\text{PdCl}(\text{PPh}_3)\text{L}]$ suitable for X-ray diffraction studies were obtained from CH_3CN at room temperature. As predicted by the spectral data, $[\text{PdCl}(\text{PPh}_3)\text{L}]$ has a monomeric square-planar structure in which Schiff base ligand is coordinated to palladium metal via the azomethine nitrogen and thiolate sulfur atoms, forming one stable five membered metallacycle [containing atoms $\text{Pd}(1)/\text{S}(2)/\text{C}(25)/\text{N}(2)/\text{N}(1)$]. This ring obtained from chelating of the *S*-allyl β -*N*-(benzylidene)dithiocarbazate ligand $[\text{L}]^-$, of type Pd-NNCS , is essentially planar. The NS ligand is coordinated in its deprotonated thiolate form. The remaining coordination sites are occupied by triphenylphosphine [*trans* to $\text{N}(1)$] and chlorine atom [*trans* to $\text{S}(2)$]. Then $\text{Pd}(\text{II})$ has an NSPCl coordination environment. The relevant bond lengths and bond angles are given in Table 2. The ORTEP diagram of the complex is shown in Figure 1. The intermolecular distance between Pd atoms of consecutive molecules in the packing is 8.798 Å. The $\text{C}(25)–\text{S}(2)$ bond length is 1.739 Å, which is shorter than 1.82 Å for a C–S single bond and longer than 1.56 Å for a C=S double bond.²¹ The C–N bond distance, $\text{C}(25)–\text{N}(2)$ 1.279 Å, conforms to the double bond [$d(\text{C}=\text{N})$ 1.28 Å].²¹ The Pd–S distance, 2.250 Å, is in the range normally found in four-coordinate $\text{Pd}(\text{II})$ complexes of sulfur-nitrogen chelating agents.^{8,22} The Pd–N distances are also com-

parable with the values found in most square-planar palladium(II) complexes of Schiff base ligands derived from thiosemicarbazid and *S*-alkyl esters of dithiocarbazic acid^{8,22} and other *N*-substituted derivatives¹¹ of dithiocarbazates.

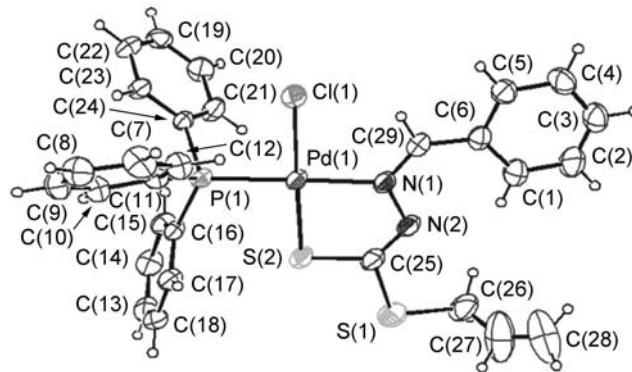


Figure 1 An ORTEP drawing of complex $[\text{PdCl}(\text{PPh}_3)\text{L}]$ with the atom labeling scheme (50% probability thermal ellipsoids).

Table 2 Selected bond lengths (Å) and angles (°) for $[\text{PdCl}(\text{PPh}_3)\text{L}]$

$\text{Pd}(1)–\text{N}(1)$	2.098(0)	$\text{N}(1)–\text{Pd}(1)–\text{S}(2)$	83.21(3)
$\text{Pd}(1)–\text{S}(2)$	2.250(2)	$\text{N}(1)–\text{Pd}(1)–\text{P}(1)$	171.46(7)
$\text{Pd}(1)–\text{P}(1)$	2.255(7)	$\text{N}(1)–\text{Pd}(1)–\text{Cl}(1)$	95.49(4)
$\text{Pd}(1)–\text{Cl}(1)$	2.343(9)	$\text{S}(2)–\text{Pd}(1)–\text{P}(1)$	92.43(2)
$\text{N}(1)–\text{N}(2)$	1.406(6)	$\text{S}(2)–\text{Pd}(1)–\text{Cl}(1)$	178.06(3)
$\text{N}(1)–\text{C}(29)$	1.287(1)	$\text{P}(1)–\text{Pd}(1)–\text{Cl}(1)$	89.03(3)
$\text{N}(2)–\text{C}(25)$	1.278(9)	$\text{C}(25)–\text{N}(2)–\text{N}(1)$	112.79(7)
$\text{C}(25)–\text{S}(2)$	1.738(7)	$\text{S}(2)–\text{C}(25)–\text{S}(1)$	110.67(3)
$\text{C}(25)–\text{S}(1)$	1.750(7)	$\text{N}(2)–\text{C}(25)–\text{S}(1)$	121.57(7)
$\text{S}(1)–\text{C}(26)$	1.798(1)	$\text{C}(25)–\text{S}(1)–\text{C}(26)$	105.43(9)
$\text{C}(26)–\text{C}(27)$	1.432(7)	$\text{S}(1)–\text{C}(26)–\text{C}(27)$	113.39(0)
$\text{C}(27)–\text{C}(28)$	1.173(8)	$\text{C}(26)–\text{C}(27)–\text{C}(28)$	143.44(3)

The palladium-nitrogen bond length in the metallacycle, 2.098(0) Å, is longer than the predicted single bond value of 2.011 Å, based on the sum of covalent radii for nitrogen (sp^2) and palladium, 0.701 and 1.31 Å, respectively,²³ reflecting the *trans* influence of the phosphorus atom.²⁴ The Pd–P bond distance, 2.255(7) Å, is shorter than the sum of the single bond radii of palladium and phosphorus (2.41 Å), suggesting partial double bond character similar to the others reported earlier.^{25,26} The Pd–Cl bond length, 2.343(9) Å, is consistent with Pd–Cl distances found in related species.^{26,27}

The highest deviation from the least squares plane in $\text{Pd}(\text{II})$ coordination environment was observed for P(1) atom by 0.325 Å. The angles of $\text{N}(1)–\text{Pd}(1)–\text{P}(1)$ and $\text{S}(2)–\text{Pd}(1)–\text{Cl}(1)$ have not the ideal value of 180° (171.47° and 178.06°). The other four angles subtended at the $\text{Pd}(\text{II})$ ion all deviate from the values expected for an ideal square-planar geometry (See Table 2). Com-

parison between bond angles of $[\text{PdCl}(\text{PPh}_3)\text{L}]$ complex with those of other related square-planar palladium(II) complexes of similar ligands²² shows that the distortion is a common phenomenon in square-planar-Pd(II) complexes of NS donor ligands.

Decoding of intermolecular interactions: Hirshfeld surface and fingerprint plot

Exploring crystal lattice with Hirshfeld surfaces and fingerprint plots produced with CrystalExplorer computer program using the structural information obtained from X-ray diffraction determination is presented in this section. Particular attention is given to 3D shape and curvature surfaces and breakdown of fingerprint plots which provide a concise summary of the intermolecular interactions occurring in the crystal by mapping the fraction of points on the corresponding Hirshfeld surface as a function of the closest distances from the point to nucleus interior (d_i) and exterior (d_e) to the surface. The Hirshfeld surfaces for $[\text{PdCl}(\text{PPh}_3)\text{L}]$ are shown in

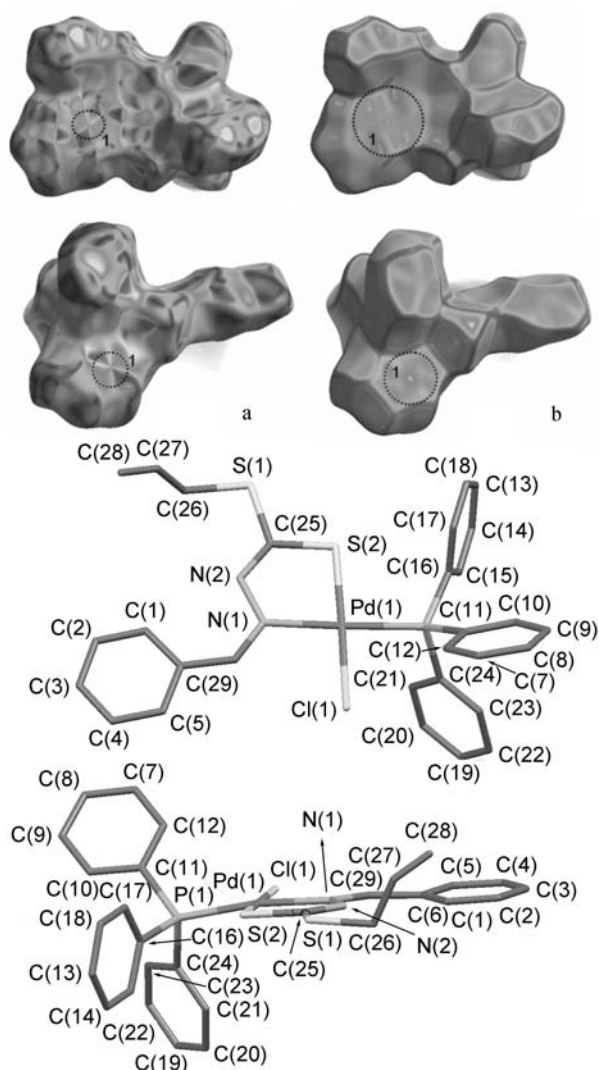


Figure 2 Hirshfeld surface of $[\text{PdCl}(\text{PPh}_3)\text{L}]$, mapped with shape index (a) and curviness property (b) in two orientations. The molecular structures have been added right hand to the Hirshfeld surface maps for presenting more clear geometry.

Figure 2.

$\pi\cdots\pi$ interactions are evident on the Hirshfeld surface as a large flat region across the molecule, which is most clearly visible on the curviness surfaces. The pattern of red and blue triangles on the same region of the shape index surface is another characteristic of $\pi\cdots\pi$ interactions. Blue triangles represent convex regions due to ring carbon atoms of the molecule inside the surface, while red triangles represent concave regions due to carbon atoms of the π -stacked molecule above it. As mentioned above, over the plane of the molecule, inspection of the adjacent red and blue triangles on the shape index surfaces and large flat region on the curviness surfaces of $[\text{PdCl}(\text{PPh}_3)\text{L}]$ shows the $\pi\cdots\pi$ stacking (see the regions labeled 1 in Figure 2) in which the shortest one has the distance of 3.672 Å formed between C(7)—C(12) π -rings with symmetry code (x, y, z). By using breakdown of fingerprint plot technique, we can decompose fingerprint plots to highlight intermolecular contacts. This disintegration allows the separation of contributions from different interaction kinds, which commonly overlap in the full fingerprint or difficultly, has been recognized in 3D maps.

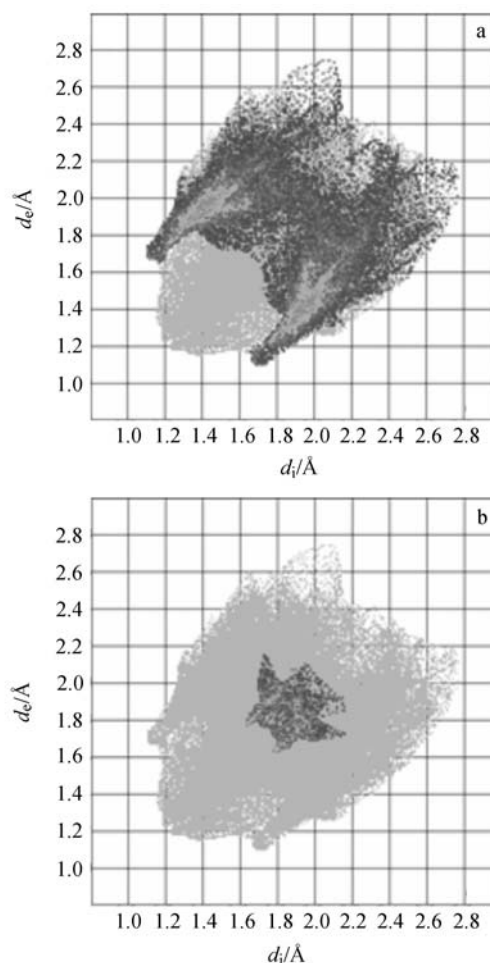


Figure 3 Fingerprint plots for $[\text{PdCl}(\text{PPh}_3)\text{L}]$ resolved into C—H... π (a) and N... π (b) contacts. The full fingerprint appears beneath each decomposed plot as a grey shadow.

Figure 3 showed highlighting separately the C—H $\cdots\pi$ and N $\cdots\pi$ intermolecular contacts on fingerprint plot.

To provide a context, the outline of the full fingerprint is shown in grey. The C—H $\cdots\pi$ interaction formed between C(22)—H(22A) and C(19)—C(24) phenyl rings of triphenylphosphine with the bond length 2.860 Å, constitutes an intermolecular dimer (Figure 4). Each dimer interacts with a neighboring dimeric unit by N $\cdots\pi$ interactions between the N(2) atoms and phenyl rings of *S*-allyl dithiocarbazate Schiff bases, 3.636 Å, to form a one dimensional chain (see the region labelled (b) in Figure 5).

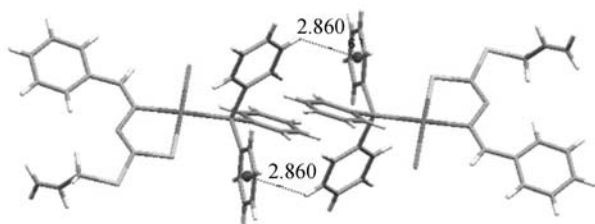


Figure 4 Dimer unit formed via the C—H $\cdots\pi$ interactions.

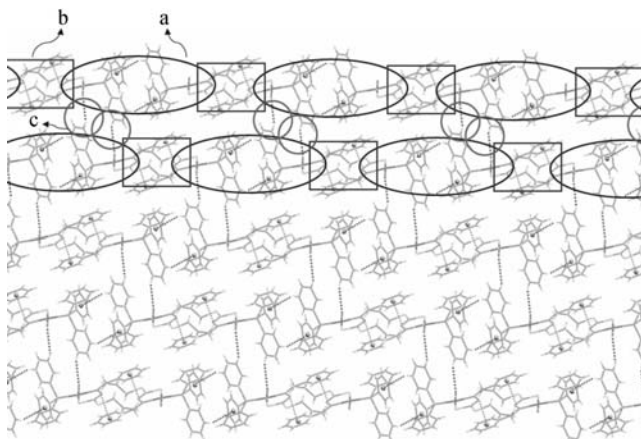


Figure 5 A view shows assemblage of [PdCl(PPh₃)L] via C—H $\cdots\pi$ interactions and formation of dimer unit (a) and N $\cdots\pi$ contacts and connection of dimer unit (b) which have made 1D chain and finally, Cl \cdots H interactions (c) that link parallel chains to make an infinite sheet.

In the same manner, Figure 6 represents the selective highlighted C—H \cdots Cl intermolecular contacts on d_{norm} surface¹⁶ and fingerprint plot, C(20)—H(20A) \cdots Cl(1) 2.948 Å. The shortest distances have been normalized with respect to the van der Waals radii of the atoms. In the color scale, blue regions have no contacts shorter than the van der Waals radii, red regions are closer than the van der Waals radii and white regions are a distance equal to the sums of appropriate radii. Cl \cdots H interactions connect the one dimensional chains to create an infinite sheet (Figure 5). Figure 7 illustrates selective highlighted weak C—H \cdots S intermolecular contacts on fingerprint plot of title complex, C(22)—H(22A) \cdots S(1) 3.047 Å. To provide a context, the outline of the full

fingerprint is shown in grey $\pi\cdots\pi$ and C—H \cdots S intermolecular interactions link the infinite sheet to form a three-dimensional network to be shown in Figure 8.

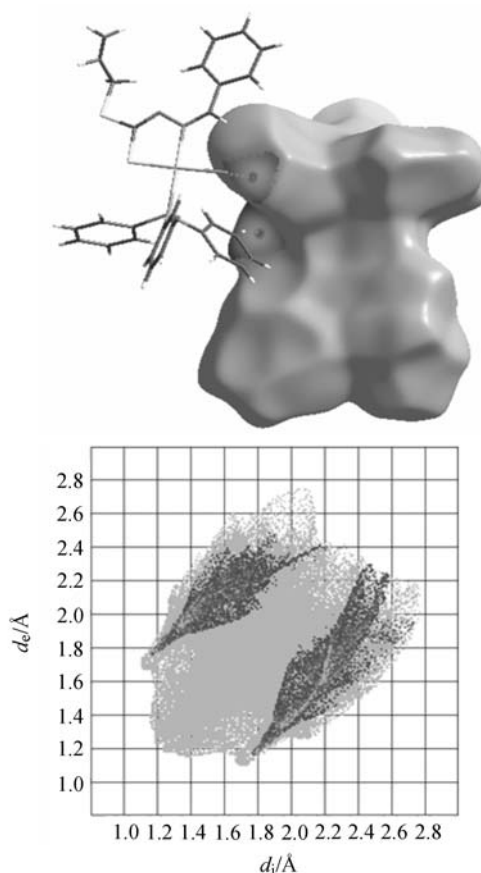


Figure 6 Selective highlighting of Cl \cdots H and H \cdots Cl contacts on the d_{norm} surface and fingerprint plot of [PdCl(PPh₃)L]. The full fingerprint appears beneath each decomposed plot as a grey shadow.

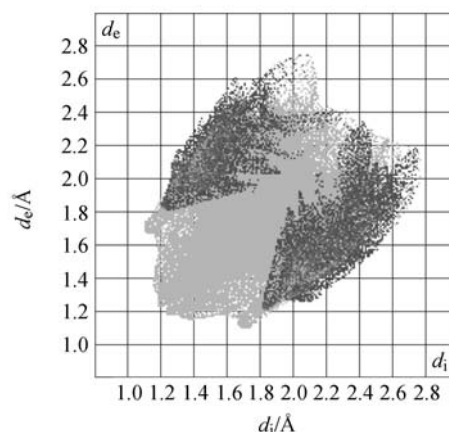


Figure 7 Fingerprint plot for [PdCl(PPh₃)L] resolved into C—H \cdots S contacts. The full fingerprint appears beneath each decomposed plot as a grey shadow.

Conclusion

In conclusion, we have prepared NS-donor bidentate

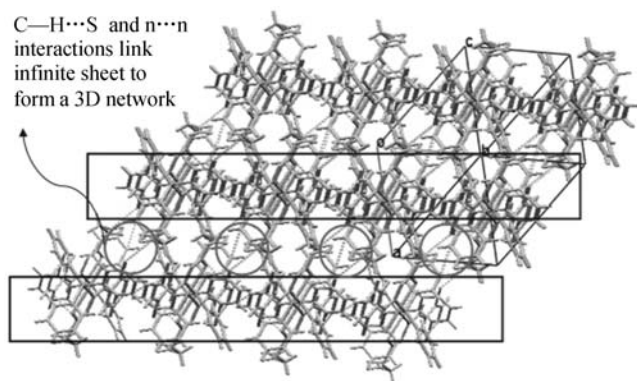


Figure 8 Representation of a 3-D network of $[\text{PdCl}(\text{PPh}_3)\text{L}]$.

S-allyldithiocarbazate Schiff base ligand and its $[\text{PdCl}(\text{PPh}_3)\text{L}]$ mixed ligand complex, as first example of complexation of Pd(II) with *S*-allyl dithiocarbazate Schiff base. The synthesized ligand and its complex have been characterized by spectrometric methods and X-ray single crystal diffraction. Crystal structure determination shows that L acts as a mono-negatively charged NS-bidentate ligand which coordinated to the metal ion via the deprotonated amidate nitrogen and thione sulfur atoms, forming one stable five membered metallacycle. The other remaining coordination sites, to form distorted square planar geometry for Pd(II), are occupied by triphenylphosphine [*trans* to N(1)] and chlorine atom [*trans* to S(2)]. Decoding of intermolecular interactions using Hirshfeld surface analysis, showed the presence of $\pi\cdots\pi$, $\text{N}\cdots\pi$, $\text{C—H}\cdots\pi$, $\text{Cl}\cdots\text{H}$ and weak $\text{C—H}\cdots\text{S}$ interactions in crystal lattice, which are responsible for forming a three-dimensional network.

Acknowledgements

The authors are grateful to Ferdowsi University of Mashhad and Northeast Normal University of China for providing the possibilities of doing this research.

References

- (a) Mohan, M.; Kumar, M.; Kumar, A.; Madhuranath, P. H.; Jha, N. K. *J. Inorg. Biochem.* **1988**, 33, 121.
(b) Das, M.; Livingstone, S. E. *Brit. J. Cancer.* **1988**, 37, 466.
(c) Chew, K. B.; Tarafder, M. T. H.; Crouse, K. A.; Ali, M. A.; Yamin, B. M.; Fun, H. K. *Polyhedron* **2004**, 23, 1385.
- (a) Singh, R. V.; Chaudhary, P.; Chauhan, S.; Swami, M. *Spectrochim. Acta Part A* **2009**, 72, 260.
(b) Crouse, K. A.; Chew, K. B.; Tarafder, M. T. H.; Kasbolah, A.; Ali, M. A.; Yamin, B. M.; Fun, H. K. *Polyhedron* **2004**, 23, 161.
(c) Bi, S. W.; Li, G. Z. *Synth. React. Inorg. Met. Org. Chem.* **1999**, 29, 1829.
- (a) Shailendra, S.; Bharti, N.; Naqvi, F.; Azam, A. *Helv. Chim. Acta* **2002**, 85, 2713.
(b) Bharti, N.; Maurya, M. R.; Naqvi, F.; Bhattacharya, A.; Bhattacharya, S.; Azam, A. *Eur. J. Med. Chem.* **2000**, 35, 481.
- (a) Hatta, R.; Sumina, I.; Kinugawa, J.; Tamura, B.; Yamamoto, H.; Suzuki, S. *BR 963924* [*Chem. Abstr.* **1964**, 61, 99870].
(b) Koromogawa, J.; Tamura, B. *JP 19114*, **1963**.
- Frausto da Silva, J.; Williams, R. *The Biological Chemistry of the Elements*, Clarendon Press, Oxford, **1991**.
- Kaim, W.; Schwederski, B. *Bioinorganic Chemistry: Inorganic Elements in the Chemistry of Life*, Wiley, New York, **1996**.
- Coughlin, P. K.; Lippard, S. J. *J. Am. Chem. Soc.* **1984**, 106, 2328.
- Zhou, H. P.; Li, D. M.; Wang, P.; Cheng, L. H.; Gao, Y. H.; Zhu, Y. M.; Wu, J. Y.; Tian, Y. P.; Tao, X. T.; Jiang, M. H.; Fun, H. K. *J. Mol. Struct.* **2007**, 826, 205.
- Ali, M. A.; Livingstone, S. E.; Phillips, D. J. *Inorg. Chim. Acta* **1971**, 5, 119.
- (a) Wang, X. Y.; Deng, Z. X.; Jin, B. K.; Tian, Y. P.; Lin, X. Q. *Spectrochim. Acta Part A* **2002**, 58, 3113.
(b) Wang, X. Y.; Deng, Z. X.; Jin, B. K.; Tian, Y. P.; Lin, X. Q. *Bull. Chem. Soc. Jpn.* **2002**, 75, 1669.
- Bonamico, M.; Fares, V.; Petrilli, L.; Tarli, F.; Chiozzini, G.; Riccucci, C. *J. Chem. Soc., Dalton Trans.* **1994**, 3349.
- (a) Yazdanbakhsh, M.; Takjoo, R. *J. Struc. Chem.* **2008**, 19, 895.
(b) Yazdanbakhsh, M.; Heravi, M. M.; Takjoo, R.; Frank, W. Z. *Anorg. Allg. Chem.* **2008**, 634, 972.
(c) Yazdanbakhsh, M.; Hakimi, M.; Heravi, M. M.; Boese, R. Z. *Anorg. Allg. Chem.* **2006**, 632, 2201.
(d) Yazdanbakhsh, M.; Hakimi, M.; Heravi, M. M.; Ghassemzadeh, M.; Neumüller, B. Z. *Anorg. Allg. Chem.* **2005**, 631, 924.
- McKinnon, J. J.; Spackman, M. A.; Mitchell, A. S. *Acta Crystallogr. B* **2004**, 60, 627.
- (a) McKinnon, J. J.; Spackman, M. A.; Mitchell, A. S. *Chem. Eur. J.* **1998**, 4, 2136.
(b) Spackman, M. A.; Byrom, P. G. *Chem. Phys. Lett.* **1997**, 267, 215.
- Spackman, M. A.; McKinnon, J. J. *CrystEngComm.* **2002**, 4, 378.
- McKinnon, J. J.; Jayatilaka, D.; Spackman, M. A. *Chem. Commun.* **2007**, 37, 3814.
- Sheldrick, G. M. *SHELXS97 (Crystal Structure Solution) and SHELXL97 (Crystal Structure Refinement)*, University of Göttingen, Germany, **1997**.
- Tarafder, M. T. H.; Jin, K. T.; Crouse, K. A.; Ali, M. A.; Yamin, B. M.; Fun, H. K. *Polyhedron* **2002**, 21, 2547.
- Prabhakaran, R.; Renukadevi, S. V.; Karvembu, R.; Huang, R.; Mautz, J.; Huttner, G.; Subashkumar, R.; Natarajan, K. *Eur. J. Med. Chem.* **2008**, 43, 268.
- Das, S.; Pal, S. *J. Organomet. Chem.* **2004**, 689, 352 and references there in.
- Curry, J. D.; Jandacer, R. J. *J. Chem. Soc., Dalton Trans.* **1972**, 1120.
- Wu, J. Y.; Tian, Y. P.; Xie, F. X.; Ni, S. S. *Chin. Chem. Lett.* **1999**, 10, 251.
- Allen, F. H.; Kennard, O.; Watson, D. G.; Taylor, R. *J. Chem. Soc., Dalton Trans.* **1989**, S1.
- (a) Suzuki, T.; Morikawa, A.; Kashiwabara, K. *Bull. Chem. Soc. Jpn.* **1996**, 69, 2539.

- (b) Habtemariam, A.; Watchman, B.; Potter, B. S.; Palmer, R.; Parsons, S.; Parkin, A.; Sadler, P. J. *J. Chem. Soc., Dalton Trans.* **2001**, 1306.
- 25 Suarez, A.; Vila, J. M.; Gayoso, E.; Gayoso, M.; Hiller, W.; Castineiras, A.; Strahle, J. Z. *Inorg. Allg. Chem.* **1986**, 535, 213.
- 26 Bosque, R.; López, C.; Solans, X.; Font-Bardia, M. *Organometallics* **1999**, 18, 1267.
- 27 Vila, J. M.; Gayoso, M.; Fernández, A.; Adams, H.; Bailey, N. A. *J. Organomet. Chem.* **1993**, 448, 233.

(E0905011 Cheng, F.; Lu, Z.)